

The energetic of (CH₂F₂)₂ investigated by TDL IR spectroscopy and DFT computations: From collision induced relaxation of ro-vibrational transitions to non-covalent interactions

Nicola Tasinato, Arianna Turchetto, Paolo Stoppa, Andrea Pietropolli Charmet, and Santi Giorgianni

Citation: *The Journal of Chemical Physics* **142**, 134310 (2015); doi: 10.1063/1.4916911

View online: <http://dx.doi.org/10.1063/1.4916911>

View Table of Contents: <http://scitation.aip.org/content/aip/journal/jcp/142/13?ver=pdfcov>

Published by the [AIP Publishing](#)

Articles you may be interested in

[MIPAS: 10 years of spectroscopic measurements for investigating atmospheric composition](#)

AIP Conf. Proc. **1531**, 23 (2013); 10.1063/1.4804698

[Rovibrational resonance effects in collision-induced electronic energy transfer: I 2 \(E , v = 0 – 2 \) + C F 4](#)

J. Chem. Phys. **125**, 194313 (2006); 10.1063/1.2363985

[Quantum mechanical investigation of rovibrational relaxation of H 2 and D 2 by collisions with Ar atoms](#)

J. Chem. Phys. **122**, 024304 (2005); 10.1063/1.1829976

[Collisional removal of O 2 \(b 1 Σ g + , u=2,3\)](#)

J. Chem. Phys. **116**, 4877 (2002); 10.1063/1.1456026

[Temperature dependence of the collisional removal of O 2 \(b 1 Σ g + , v=1 and 2\) at 110–260 K, and atmospheric applications](#)

J. Chem. Phys. **110**, 18 (1999); 10.1063/1.478079



The energetic of (CH₂F₂)₂ investigated by TDL IR spectroscopy and DFT computations: From collision induced relaxation of ro-vibrational transitions to non-covalent interactions

Nicola Tasinato,^{a)} Arianna Turchetto, Paolo Stoppa, Andrea Pietropolli Charmet, and Santi Giorgianni

Dipartimento di Scienze Molecolari e Nanosistemi, Università Ca' Foscari Venezia, Calle Larga S. Marta 2137, I-30123 Venezia, Italy

(Received 30 January 2015; accepted 22 March 2015; published online 7 April 2015)

Difluoromethane (CH₂F₂) is an atmospheric pollutant presenting strong absorptions within the 8–12 μm atmospheric window, hence it can contribute to global warming. Its dimer, (CH₂F₂)₂, is bound through weak hydrogen bonds (wHBs). Theoretically, wHBs are of paramount importance in biological systems, though their modeling at density functional theory (DFT) level requires dispersion correlations to be accounted for. In this work, the binding energy (3.1 ± 0.5 kcal mol⁻¹) of (CH₂F₂)₂ is experimentally derived from the foreign broadening coefficients of the monomer compound, collisionally perturbed by a range of damping gases. Measurements are carried out on CH₂F₂ ro-vibrational transitions by means of tunable diode laser spectroscopy. Six stationary points on the potential energy surface (PES) of the dimer are investigated at DFT level by using some of the last generation density functionals (DFs). The Minnesota M06 suite of functionals as well as range separated DFs and DFs augmented by the non-local (NL) van der Waals (vdW) dispersion corrections are considered. DFT results are compared to reference values at the estimated complete basis set (CBS) limit of CCSD(T) theory (coupled cluster with singles and doubles augmented by a perturbational estimate of connected triples) and to the experimental binding energy. The M06-2X, M06-HF, VV10, BLYP-NL, and B3LYP-NL DFs reproduce CCSD(T)/CBS binding energies with a mean absolute deviation <0.4 kcal mol⁻¹ and about the same deviation from the experimental value. The present results are of twofold relevance: (i) they show that binding energy of homodimers can be conveniently obtained from the monomer's foreign broadening coefficients and that the correct simulation of hydrogen bonds involved in (CH₂F₂)₂ needs non-covalent interactions to be included into DFT; (ii) O₂- and N₂-pressure broadening parameters represent fundamental data for exploiting the efficacy of remote sensing measurements employed to retrieve temperature and concentration profiles of our atmosphere. © 2015 AIP Publishing LLC. [<http://dx.doi.org/10.1063/1.4916911>]

I. INTRODUCTION

The broadening of molecular spectral lines has been the subject of considerable interest to many scientists since the beginning of the twentieth century. An extended discussion can be found in the book by Hartmann *et al.*¹ In recent years, these studies have been extended to charged species² and have received renewed attention from the physical chemistry community because spectroscopic parameters are key features in the remote-sensing quantification of atmospheric constituents and trace-gas pollutants^{3–5} as well as in the interpretation of astrophysical data obtained from ground- and space-based facilities.^{6,7} Besides providing basic information for inverting these observational data, thus retrieving concentration or temperature profiles, collisional broadening and shifting parameters can shed light on the intermolecular forces driving the scattering event in the gas phase (e.g., see Refs. 8–13 and references therein).

Within this framework, in the present work, the broadening coefficients of CH₂F₂ perturbed by a range of atomic and molecular damping gases are employed for inferring the dissociation energies of the (CH₂F₂)₂ dimer. On one side, difluoromethane, belonging to the family of hydrofluorocarbons (HFCs), represents an emerging atmospheric pollutant whose atmospheric concentration has steadily grown up since 1990s, being around 3 ppt in 2005. Indeed, this molecule has been proposed as a valid replacement for both chlorofluorocarbons (CFCs) and hydrochlorofluorocarbons (HCFCs), in particular HCFC-22, which have been phased out by the Montreal protocol due their capacity of destroying the stratospheric ozone layer.

Nowadays, CH₂F₂ is widely used in refrigerant mixtures, together with CF₃CH₃, CF₃CH₂F, and CF₃CHF₂. With respect to CFCs and HCFCs, hydrofluorocarbons, being chlorine-free, do not contribute to the ozone loss, and further they have shorter atmospheric lifetimes, as once in the troposphere they undergo degradation by reacting toward OH radicals. Due to its atmospheric interest and also because it received attention as an efficient laser medium for the generation of strong far infrared (FIR) laser lines when optically pumped by CO₂

^{a)} Author to whom correspondence should be addressed. Electronic mail: tasinato@unive.it. Telephone: +39 041 2348598. Fax: +39 041 2348594.

lasers, CH_2F_2 has been the subject of several experimental and theoretical spectroscopic investigations (for an overview of the relevant literature, see Refs. 14–16 and references therein). Very recently, the CH_2F_2 adsorption over the TiO_2 surface, being the first step involved in gas-phase heterogeneous catalysis aimed at removing atmospheric pollutants, has been studied by coupling diffuse reflectance infrared spectroscopy to periodic quantum chemical calculations.¹⁷

The difluoromethane dimer has also been investigated experimentally and theoretically. Microwave experiments, first carried out by Caminati and co-workers¹⁸ and then refined by Blanco *et al.*,¹⁹ led to the determination of rotational and centrifugal distortion constants, from which the structure of the most stable conformer was derived, by assuming that the monomer is not affected by structural modifications upon complexation. While some years ago, the dimer was theoretically studied at HF, B3LYP, and MP2 levels of theory,²⁰ very recently, it has been deeply investigated by using dispersion corrected density functional theory (DFT-D3).²¹ The most stable structure of the homodimer is characterized by three weak-hydrogen bonds (wHBs) between F and H atoms.

Hydrogen bonds have an indisputable relevance for many chemical and biological systems, as they determine their structures and hence their functionalities. Their theoretical investigations need suitable approaches for correctly simulating and hence understanding the structure, thermochemistry, and spectroscopic properties of molecular systems featuring this kind of non-covalent interaction. Nowadays, methods rooted in density functional theory are the working option for molecules composed of hundreds to thousands of atoms and have been successfully applied in many applications. Nevertheless, it has been demonstrated that they are unable to correctly describe long-range non-covalent interactions.^{22–26} Accounting for the lack of long range correlation effects has become of fundamental importance for many practical applications of electronic structure computations. Many research efforts have therefore been spent to include London dispersion forces into standard DFT: several schemes and new density functionals (DFs) have been proposed during the last few years (for an overview, see Refs. 27 and 28, and references therein). Some of the most common and successful approaches

can be grouped into three main classes, namely, atom pairwise additive schemes,^{29,30} non-local (NL) van der Waals functionals,^{31,32} and highly parameterized functionals.^{33,34} Benchmarking their predictions against experimental or highly accurate theoretical data is of paramount importance for understanding their applicability and portability to larger systems.

Given these premises, a second aim of the present work is the theoretical investigation of the $(\text{CH}_2\text{F}_2)_2$ energetic by using some DFs capable of treating long-range interactions to compare against the experimental dissociation energy here determined and that obtained from highly correlated wavefunction calculations.

The work is structured as follows: computational and experimental details are described in Secs. II and III, respectively. Results are presented and discussed in Sec. IV, and finally, conclusions are summarized in Sec. V.

II. COMPUTATIONAL METHODS

The dissociation energies of $(\text{CH}_2\text{F}_2)_2$ were computed in correspondence of the six stationary points found on its potential energy surface according to DFT-D3 computations performed in a previous work.²¹ In particular, for both the complexes and the monomers, B3LYP-D3/def2-TZVP geometries were considered. For the sake of completeness, the structures of the six hydrogen bonded CH_2F_2 dimers are reproduced in Figure 1. Besides, in that work also reference values at the estimated complete basis set (CBS) limit of CCSD(T) theory (coupled cluster with singles and doubles augmented by a perturbational estimate of connected triples) were worked out²¹ according to a consolidated two point extrapolation procedure from aug-cc-pVTZ and aug-cc-pVQZ basis sets.

In the present work, we turned our attention on different density functionals of the last generation, which have been developed to provide high accuracy for thermochemical data and possibly to take into account long range correlation effects such as London dispersion interactions. In particular, the functionals belonging to the Minnesota M06 suite³⁴ (namely, M06 and M06-2X,³⁴ M06-L,³⁵ and M06-HF³⁶) were

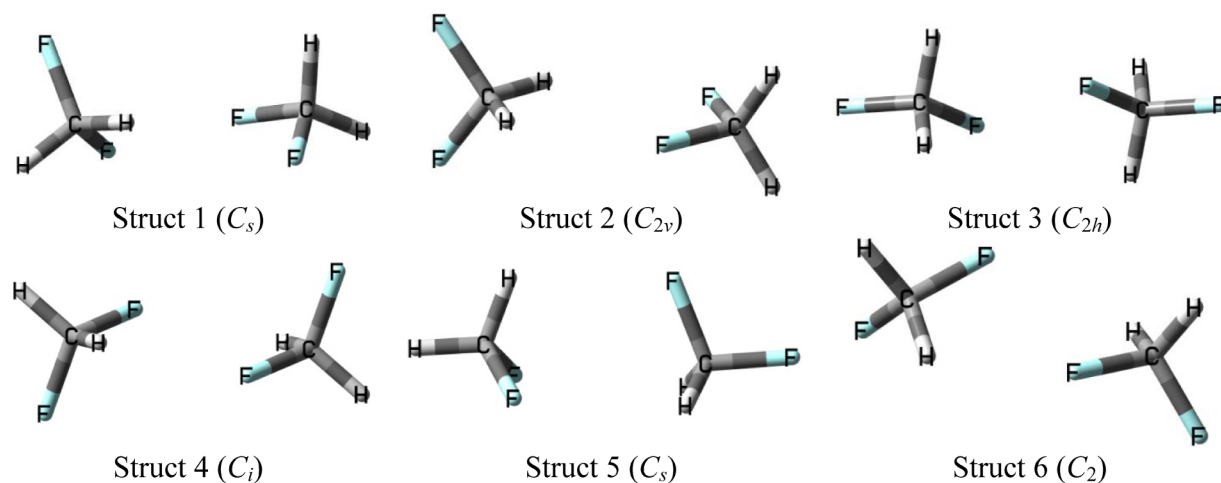


FIG. 1. Structures of the six stationary points on the PES of $(\text{CH}_2\text{F}_2)_2$ (point group symmetry is indicated within parentheses).

considered, as well as the range separated CAM-B3LYP,³⁷ LC- ω PBE,³⁸ and ω B97X-D,³⁹ the latter also including empirical corrections for dispersion energies. Further, the NL van der Waals functional approach, recently developed by Vydrov and Van Voorhis,³² has been considered. This route for the inclusion of long range correlation uses only the electron density to compute the non-local contribution and treats inter- and intra-molecular dispersion interactions on equal footing. The NL contribution was combined with three GGA (Generalized Gradient Approximation) functionals (namely, rPW86PBE,^{40–42} BLYP,^{43,44} and revPBE^{42,45}) and the hybrids B3LYP,^{44,46} B3PW91,^{46,47} revPBE0,^{45,48,49} and revPBE38,^{30,40} which have been recently tested for either the thermochemical properties or structural parameters.⁵⁰ Actually, rPW86PBE-NL coincides with the VV10 functional, originally devised by Vydrov and Van Voorhis.

In order to test eventual basis set dependences of the selected DFT methods, computations were carried out by using basis sets of either triple- or quadruple- ζ quality belonging to Pople's,^{51–53} Dunning's,^{54–57} or Ahlrichs'^{58–60} families. In more detail, among triple- ζ basis sets, 6-311++G(*d,p*), aug-cc-pVTZ, and def2-TZVP basis functions were adopted, while aug-cc-pVQZ and def2-QZVP were selected as quadruple- ζ basis sets. Some computations were also carried out by using the cc-pVnZ ($n = T, Q$) bases, yet these gave results (almost) coincident to those of their augmented versions.

For the M06 family and the range separated functionals, computations were performed by using the Gaussian 09 suite of programs,⁶¹ while the ORCA software^{62,63} was employed for the calculations adopting the NL DF approach. For the latter, the resolution of identity approximations RI-J⁶⁴ and RI-JK^{65,66} was employed for GGA and hybrid functionals, respectively, with auxiliary basis sets taken from the ORCA library.

In all cases, (CH₂F₂)₂ energies were corrected for the basis set superposition error (BSSE) according to the counterpoise (CP) procedure proposed by Boys and Bernardi.⁶⁷ As expected, for a quadruple- ζ basis set, the CP correction resulted in a small contribution, in general lower than 0.1 kcal mol⁻¹, these large bases giving results quite close to the Kohn-Sham-limit.

III. EXPERIMENTAL DETAILS

CH₂F₂ high resolution IR spectra were recorded within the atmospheric window, around 8 μ m, by using a tunable diode laser spectrometer.^{68–70} For the present measurements, the instrument was operating in a three beam configuration in which the radiation emitted by the source is split into three different beams. One of these passed through the 68.2 (\pm 0.2) cm absorption cell containing the CH₂F₂ sample, while the two other beams were, respectively, sent to a Germanium etalon and a second cell filled with SO₂, both employed for calibration purposes. The three beams were then collected by three different HgCdTe detectors cryogenically cooled at liquid nitrogen temperature and acquired at 12.5 MS s⁻¹ by a four channel ultrafast digitizer card with a 14 bit vertical resolution. Two different commercial lead salt lasers, centered at 8.2 and 8.1 μ m, respectively, were employed and fine

wavelength tuning was achieved by sweeping their injection current at fixed temperature.

CH₂F₂ foreign-broadening measurements were carried out at room temperature (296 ± 2 K), by perturbing the radiating species by He, Ne, and Ar noble gases as well as by N₂ and O₂ molecules, according to a well established procedure.^{15,71} During these experiments, the CH₂F₂ partial pressure was kept fixed at 100 Pa, depending on the intensity of the spectral lines, and increasing quantities of damping gas were added up to total pressures of 40 hPa. An elapsed time of 10 min between the filling of the cell and the recording of the spectra was adopted in order to promote gas homogenization. In order to increase the accuracy of the retrieved parameters, for each collision partner, two independent series of measurements were performed. The CH₂F₂ sample was used without any further purification as supplied by Aldrich with a stated purity of 99.7%.

The acquired spectral micro windows, about 0.3 cm⁻¹ wide, were wavenumber calibrated by using the frequency of SO₂ reference lines measured from the high resolution FT-IR spectrum, resulting in a calibration accuracy of ca. 4×10^{-4} cm⁻¹; the transmittance spectra were then obtained by fitting the baseline to a polynomial function.^{68,69} The lineshape analysis was performed by using the Visual LineShape Fitting program running in multiline mode.⁷²

IV. RESULTS AND DISCUSSION

A. CH₂F₂ foreign broadening coefficients and experimental dissociation energy of (CH₂F₂)₂

The CH₂F₂ ro-vibrational transitions recorded for the lineshape analysis belong to the ν_7 normal mode, which is located at about 1178.7 cm⁻¹, within the atmospheric region, and corresponds to the CH₂ rocking vibration.¹³ Line-by-line parameters have been retrieved by simultaneously fitting all lines appearing in a given spectral micro-window to the Voigt model, while spectra recorded at different pressures were fitted independently from each other. During the fits, resonant frequencies, collisional (i.e., Lorentzian) half-widths, and line intensities were refined, while the Gaussian half-widths were constrained to the molecular value ($\gamma_{\text{CH}_2\text{F}_2}^D \approx 1.03 \times 10^{-3}$ cm⁻¹ for the transitions of interest), the instrumental lineshape function of the lasers employed being a Lorentzian. As it can be observed from the good residuals of Figure 2, presenting the spectral region between 1197.80 and 1198.25 cm⁻¹ perturbed by the different buffer gases, the Voigt profile reproduces the observed line shapes accurately, even considering the very challenging spectral congestion, with about 45 lines/cm⁻¹. The use of more refined line shape models (including, e.g., Dicke narrowing or speed dependent effects¹) does not provide any significant improvement over the Voigt function, as pointed out in a previous work.¹⁵ Strictly speaking, the Voigt profile provides a very satisfactory description of recorded transitions (at the employed experimental conditions) and further it offers a favorable computational cost.

For each transition, and each buffer gas, CH₂F₂-foreign broadening coefficients (γ_X^0 , X = He, Ne, Ar, O₂, N₂) were derived by fitting the Lorentzian half widths obtained from

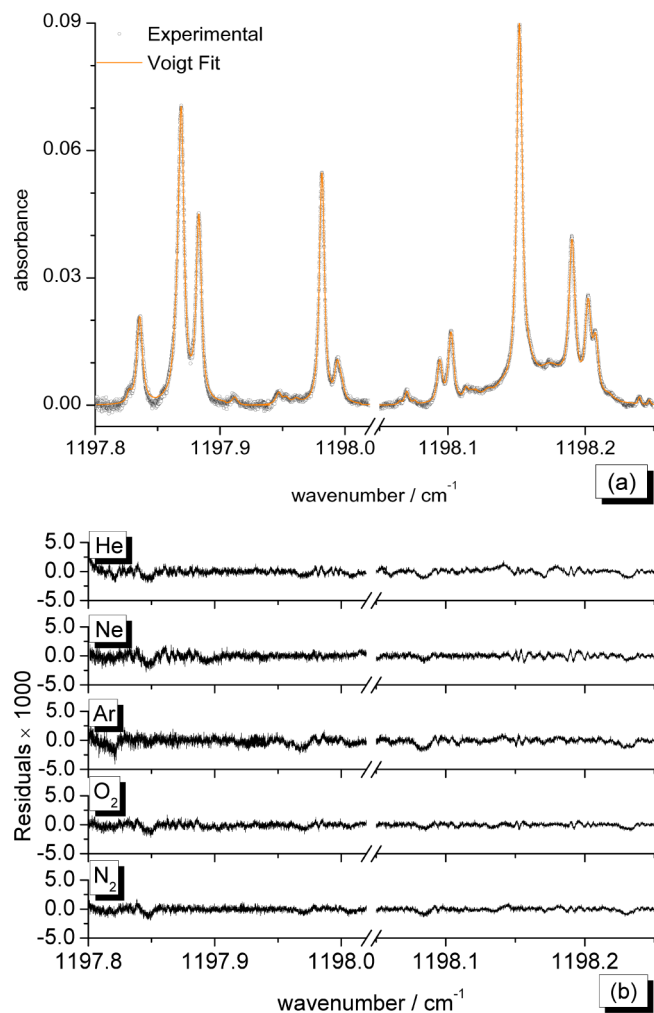


FIG. 2. (a) High resolution IR spectrum of CH_2F_2 between 1197.80 and 1198.25 cm^{-1} perturbed by similar amounts of the damping gases, and corresponding fit employing the Voigt model (experimental conditions: CH_2F_2 pressure ~ 106 Pa; optical path = 68.2 cm; $T = 295$ K). (b) Residuals of the lineshape analysis when CH_2F_2 is perturbed by He ($P_{\text{He}} = 1580$ Pa); Ne ($P_{\text{Ne}} = 961$ Pa); Ar ($P_{\text{Ar}} = 1134$ Pa); O_2 ($P_{\text{O}_2} = 1079$ Pa); N_2 ($P_{\text{N}_2} = 1110$ Pa).

the line shape analysis (Γ_L) against the partial pressure of the buffer gas (P_X), according to the following equation:

$$\Gamma_L = \Gamma_0 + \gamma_X^0 \times P_X, \quad (1)$$

where the intercept Γ_0 takes into account both the self broadening contribution and the broadening due to the instrumental apparatus. During these linear fits, the half widths were weighted according to their errors obtained from the line profile analysis. In order to combine together the two independent series of measurements performed, a double fitting procedure was adopted:⁷³ for each repetition, the value of the intercept Γ_0 was subtracted from each Γ_L thus obtaining a normalized Lorentzian half width Γ_{NL} . Subsequently, for each perturber, all the normalized half widths so obtained were employed in a second linear fit in order to obtain the final value of the foreign broadening coefficient,

$$\Gamma_{\text{NL}} = \gamma_X^0 \times P_X. \quad (2)$$

An example of such a linear fitting procedure is presented in Figure 3 for different buffer gas broadenings of the $11_{5,6} \leftarrow 10_{4,6}$

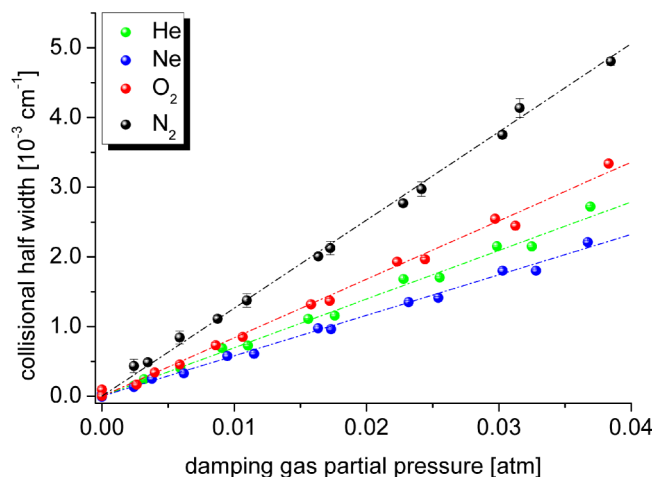


FIG. 3. Dependence of the (normalized) collisional half widths on the damping gas partial pressure for the $11_{5,6} \leftarrow 10_{4,6}$ ro-vibrational transition of CH_2F_2 perturbed by He, Ne, O_2 , and N_2 , and corresponding linear fits (dashed dotted lines).

$10_{4,6}$ transition located at 1198.1522 cm^{-1} . The obtained CH_2F_2 foreign broadening coefficients are listed in Table I.

For each transition, the broadening coefficients were employed for retrieving the corresponding collisional cross sections, σ_X , according to

$$\sigma_X = 2\pi K_B T \gamma_X^0 v_{\text{rel}}^{-1}, \quad (3)$$

where v_{rel} represents the relative speed of the colliding partners and K_B and T are the Boltzmann constant and the absolute temperature of the measurements, respectively. Collisional cross sections, in turn, were used for deriving the dissociation energy of the $(\text{CH}_2\text{F}_2)_2$ homodimer through the so-called Parmenter-Seaver equation⁷⁴

$$\sigma_X = C e^{\left[\frac{1}{T} \left(\frac{\varepsilon(\text{CH}_2\text{F}_2)_2}{K_B} \right)^{1/2} \right] \left(\frac{\varepsilon_{XX}}{K_B T} \right)^{1/2}}, \quad (4)$$

where C is a constant and $\varepsilon(\text{CH}_2\text{F}_2)_2$ and ε_{XX} are the well depths of the dimer of the radiating species and the buffer gas, respectively; the last ones can be found tabulated in the original work.⁷⁴ Although the Parmenter–Seaver equation represents an approximate relationship, it has been shown to hold for a variety of energy transfer processes, provided that attractive forces dominate the interaction.

To the best of our knowledge, up to now, it has been applied for determining the dissociation energies of $(\text{H}_2\text{CO})_2$ ⁷⁵ and $(\text{N}_2\text{O})_2$,⁷⁶ and more recently $(\text{SO}_2)_2$ ²¹ from the foreign broadening coefficients of the corresponding monomers.

For each transition analyzed, a value of the $(\text{CH}_2\text{F}_2)_2$ dissociation energy was obtained through linear fits of the logarithm of the collisional cross sections for $\text{CH}_2\text{F}_2\text{--}X$ collisions, against the well depth of the dimer X_2 . This procedure is exemplified in Figure 4 reporting $\ln \sigma_X$ as a function of $(\varepsilon_{XX}/K_B T)^{1/2}$ for different ro-vibrational transitions, together with an example of linear fit. At this point, it should be noted that for three transitions ($15_{4,12} \leftarrow 14_{3,12}$, $33_{8,25} \leftarrow 33_{7,27}$, and $32_{8,24} \leftarrow 32_{7,26}$), the nitrogen broadening coefficient appeared too high with respect to the remaining ones. This behavior has already been reported for the (H_2CO) molecule,⁷⁵ and it may

TABLE I. He-, Ne-, Ar-, O₂-, and N₂- broadening coefficients (cm⁻¹ atm⁻¹) obtained for ν₇ band ro-vibrational transitions of CH₂F₂.^a

<i>J'</i>	<i>K'_a</i>	<i>K'_c</i>	<i>J''</i>	<i>K''_a</i>	<i>K''_c</i>	γ _{He} ⁰	γ _{Ne} ⁰	γ _{Ar} ⁰	γ _{N₂} ⁰	γ _{O₂} ⁰
6	6	0	5	5	0	0.060 ₃ (1 ₁)	0.044 ₂₄ (3 ₂)	0.069 ₁ (3 ₂)	0.098 ₂ (2 ₄)	0.0728 ₀ (8 ₉)
11	5	6	10	4	6	0.0697 ₄ (9 ₇)	0.0580 ₈ (6 ₆)	0.070 ₃ (2 ₃)	0.126 ₅ (1 ₂)	0.0789 ₁ (9 ₂)
15	4	12	14	3	12	0.051 ₉ (1 ₂)	0.052 ₀ (3 ₀)	0.064 ₈ (5 ₆)	0.115 ₀ (4 ₀)	0.072 ₀ (1 ₆)
16	4	12	15	3	12	0.071 ₂ (1 ₂)	0.064 ₈ (1 ₁)	0.089 ₀ (1 ₄)	0.133 ₆ (1 ₉)	0.0850 ₁ (9 ₉)
18	3	16	17	2	16	0.064 ₅ (1 ₅)	0.055 ₈ (1 ₃)	0.0618 ₆ (1 ₃)	0.111 ₅ (1 ₄)	0.073 ₈ (1 ₁)
20	11	9	19	10	9	0.0625 ₁ (9 ₃) ^b	0.0506 ₈ (7 ₁) ^b	0.0631 ₂ (6 ₀) ^b	0.094 ₄ (2 ₁) ^c	0.071 ₄ (2 ₅) ^c
21	2	19	20	1	19	0.0633 ₃ (5 ₃)	0.0534 ₉ (9 ₅)	0.0753 ₆ (4 ₆)	0.118 ₃ (1 ₃)	0.0760 ₃ (3 ₇)
25	10	15	24	9	15	0.0762 ₅ (5 ₅) ^b	0.0511 ₁ (5 ₀) ^b	0.0724 ₄ (9 ₉) ^b	0.090 ₈ (7 ₂) ^c	0.073 ₃ (2 ₁) ^c
30	9	21	29	8	21	0.0683 ₀ (9 ₉) ^b	0.0559 ₆ (1 ₄) ^b	0.0748 ₄ (8 ₈) ^b	0.090 ₉ (8 ₃) ^c	0.072 ₃ (4 ₂) ^c
32	8	25	32	7	25	0.072 ₂ (1 ₃)	0.059 ₃ (1 ₄)	0.078 ₈ (1 ₆)	0.115 ₂ (2 ₄)	0.0816 ₁ (9 ₁)
32	8	24	32	7	26	0.062 ₁ (1 ₁)	0.046 ₁ (2 ₁)	0.079 ₂ (2 ₈)	0.126 ₈ (3 ₀)	0.073 ₅ (2 ₆)
33	8	26	33	7	26	0.042 ₄ (2 ₇)	0.036 ₉ (1 ₀)	0.060 ₄ (2 ₇)	0.087 ₂ (2 ₉)	0.0492 ₅ (6 ₄)
33	8	25	33	7	27	0.059 ₅ (1 ₄)	0.048 ₂ (1 ₈)	0.070 ₅ (2 ₂)	0.112 ₁ (3 ₇)	0.072 ₂ (1 ₂)
34	8	26	34	7	28	0.045 ₄ (1 ₇)	0.034 ₄ (1 ₃)	0.059 ₄ (1 ₇)	0.094 ₉ (3 ₀)	0.074 ₀ (1 ₁)

^aFigures in parentheses represent one standard deviation.^bFrom Ref. 21.^cFrom Ref. 15.

be due to the higher quadrupole moment of the N₂ molecule, which gives rise to a stronger electrostatic attraction with the large dipole of CH₂F₂. In such instances, the N₂-broadening coefficients have been discarded from the linear interpolations. The final value of 3.1₂(±0.5₄) kcal mol⁻¹ for the dissociation energy of (CH₂F₂)₂ has been obtained by a weighted average of the values obtained from each investigated ro-vibrational transition. This value coincides with the dissociation energy obtained from the analysis of a smaller number of ro-vibrational transitions (2.8 ± 0.3 kcal mol⁻¹).²¹

B. Theoretical (CH₂F₂)₂ dissociation energies from first principles DFT modeling

The dissociation energies computed for the six different stationary points on the potential energy surface (PES) of (CH₂F₂)₂ at the different levels of theory are reported in Table

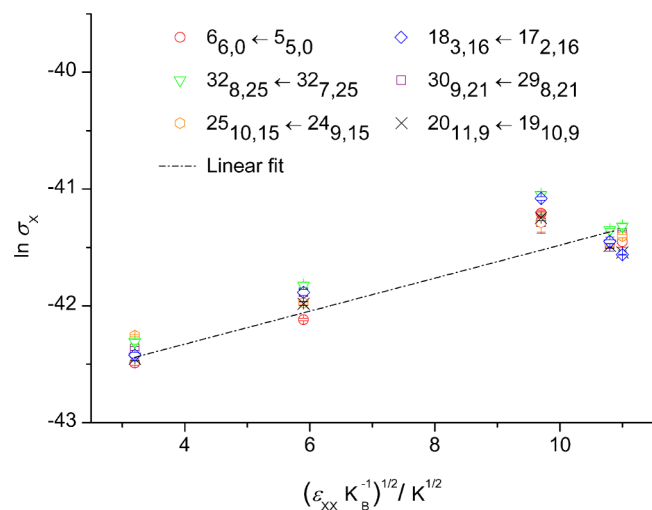


FIG. 4. Plot of $\ln(\sigma_X)$ against the dissociation energy of the He, Ne, N₂, O₂, and Ar dimers for six ro-vibrational transitions of CH₂F₂ and example of linear fit for retrieving (CH₂F₂)₂ dissociation energy. For clarity, results from only six transitions are plotted.

SI of the supplementary material,⁷⁷ together with the corresponding reference values at the estimated CCSD(T)/CBS level. The performances of the different DFT methods in evaluating the dissociation energies of (CH₂F₂)₂, assessed against the CCSD(T)/CBS ones, are illustrated in Figure 5 showing the MADs (Mean Absolute Deviations) evaluated over the six conformers. As Dunning's basis sets behave very similar to those of Ahlrichs having analogous size, the results worked out with the aug-cc-pVnZ bases are not reported.

One can readily note that the poorest agreement to the estimated CCSD(T)/CBS results is provided by M06, M06-L, and LC-ωPBE which reach MADs up to 1.3 kcal mol⁻¹. This is possibly due to the missing stabilization provided by dispersion interactions. It is also interesting to observe that with a few exceptions (actually three: M06-HF, VV10, and B3LYP-NL), the 6-311++G(*d,p*) basis set provides better results than those of Dunning and Ahlrichs, to the extent that the Pople style contraction halves their MADs in the case

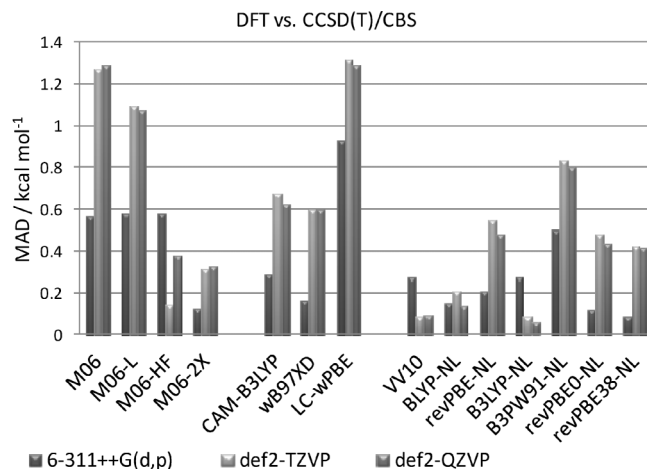


FIG. 5. Mean absolute deviations from estimated CCSD(T)/CBS reference data of dissociation energies computed at DFT level for the different stationary points on the PES of (CH₂F₂)₂.

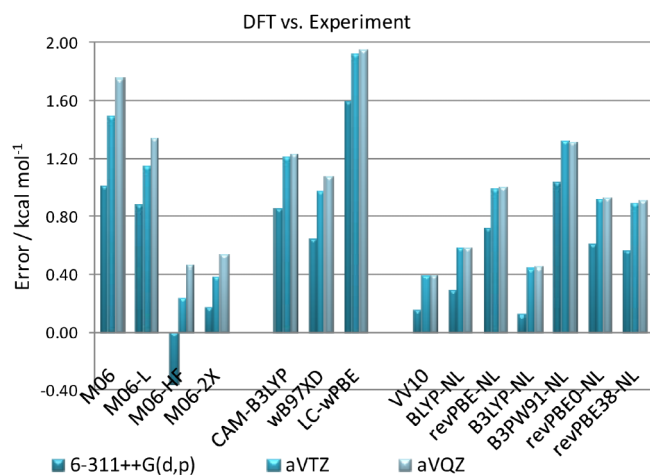


FIG. 6. Deviations from the experimental value of theoretical $(\text{CH}_2\text{F}_2)_2$ dissociation energies from DFT computations employing the 6-311++G(d, p), aug-cc-pVTZ (aVTZ), and aug-cc-pVQZ (aVQZ) basis sets.

of M06 and M06-L. Among the Minnesota DFs, M06-HF and M06-2X give a notable improvement with respect to M06 and M06-L, with MADs lower than $0.4 \text{ kcal mol}^{-1}$, but for M06-HF/6-311++G(d, p). These two meta hybrid functionals provide an accurate description of the non-covalent interactions within the $(\text{CH}_2\text{F}_2)_2$ complex. Concerning the range separated DFs, as already noted, LC- ω PBE yields the worst results, and this behaviour may be due to the cooperative effects of the missing dispersion interactions and the use of a GGA functional for the description of short range interactions. Improved energies arise when using CAM-B3LYP, since the simulation of hydrogen bonds benefits from the use of hybrid functionals, as a consequence of including a portion of Hartree-Fock exchange interaction. The last range separated DF, ω B97X-D, which includes empirical atom-atom dispersion corrections, behaves slightly better than CAM-B3LYP. Finally, very good results are provided by the non-local vdW functional approach, in particular when rPW86PBE, BLYP, and B3LYP are employed as the underlying functional: in these cases, MADs within $0.3 \text{ kcal mol}^{-1}$ are obtained with all the basis sets employed, thus conforming the outcomes from previous benchmark studies,^{50,78} which demonstrated the very powerful skills of the non-local van der Waals functional scheme in treating short and long range correlations in a seamless fashion.

In comparing theoretical dissociation energies to the experimental one, it should be taken into account that the experiments have been carried out at room temperature, and hence they actually provide an ensemble average over the different structures available to the dimer. For this reason, it may be more appropriate to compute the Boltzmann averages of the dissociation energies obtained for the different $(\text{CH}_2\text{F}_2)_2$ conformers considered. These are reported in the last column of Table SI,⁷⁷ while Figure 6 illustrates the deviations between experimental and theoretical values for DFT computations with selected basis sets. As it can be observed, the $(\text{CH}_2\text{F}_2)_2$ dissociation energy from CCSD(T)/CBS calculations compares very nicely to the experimental counterpart, underestimating it by only $0.4 \text{ kcal mol}^{-1}$.

The agreement of DFT results to experiment mirrors the behaviour previously outlined in benchmarking interaction energies at DFT level against CCSD(T) reference data. Among the Minnesota density functionals, M06-2X and M06-HF perform very well, especially when coupled to basis sets of triple- ζ quality, with deviations within $0.4 \text{ kcal mol}^{-1}$. Conversely to the remaining functionals, for which the Dunning's triple- ζ and quadruple- ζ basis sets yield the same results (and the same also holds for the Ahlrich's def2- n ZVP bases), any of the functionals belonging to the M06 family results in a poorer agreement to the experimental value, as well as to CCSD(T) reference data, on passing from triple- to quadruple- ζ basis functions. This behaviour may be due to the existence of error compensations with the smaller basis functions, or to the fact that these functionals have been parameterized mostly by using basis sets of triple- or double- ζ quality.

For the range separated density functionals, LC- ω PBE results in too loose interaction energies (around $1.5 \text{ kcal mol}^{-1}$), underestimating the energy by almost 2 kcal mol^{-1} . The agreement gets better to CAM-B3LYP, for which deviations are around 1 kcal mol^{-1} . The incorporation of empirical dispersion corrections into range separated functionals, as implemented in ω B97X-D, improves only slightly with respect with CAM-B3LYP, although ω B97X-D reaches a satisfactory deviation of $0.65 \text{ kcal mol}^{-1}$, nearly within the uncertainty of the experimental value, when coupled to the 6-311++G(d, p) basis set.

The accord between theory and experiment in the case of the non-local vdW approach depends on the underlying functional, as clearly illustrated by Figure 6. The B3PW91-NL DF gives the poorest results with deviations around $1.2 \text{ kcal mol}^{-1}$, and all the revPBE-based functionals yield errors around 1 kcal mol^{-1} when coupled with Dunning's and Ahlrich's basis sets, while they result in smaller deviations, around $0.6 \text{ kcal mol}^{-1}$, if coupled to the Pople' style 6-311++G(d, p) basis functions. Theoretical dissociation energies in very good agreement to the experimental value are obtained with the VV10, BLYP-NL, and B3LYP-NL functionals, which underbind by $0.6 \text{ kcal mol}^{-1}$ at worst.

From the above discussion, it appears that the most effective DFT approaches in describing the binding energy of the $(\text{CH}_2\text{F}_2)_2$ dimer, and hence in correctly describing the non-covalent interactions arising in this system, are the Minnesota functionals M06-2X and M06-HF, as well as the non-local density functional approach coupled to rPW86PBE and B3LYP functionals.

At this point, it is interesting to consider the outcomes of Ref. 21, which demonstrated that the atom pairwise additive treatment of dispersion correlations, as implemented within the DFT-D3 approach, is able to compute the $(\text{CH}_2\text{F}_2)_2$ and $(\text{SO}_2)_2$ dissociation energies in agreement with the experimental value, particularly when applied to PW6B95. Before concluding, the results here obtained for the BLYP and B3LYP functionals augmented with the NL vdW approach can be directly compared to those of Ref. 21 adopting the D3 correction scheme. When used in conjunction with the same basis set (def2-TZVP), BLYP-NL yields a deviation of $0.7 \text{ kcal mol}^{-1}$ from the experiment and a MAD of $0.2 \text{ kcal mol}^{-1}$ with respect to estimated CCSD(T)/CBS data. BLYP-D3 performs slightly poorer, with a deviation of

0.9 kcal mol⁻¹ and a MAD of 0.4 kcal mol⁻¹. Concerning the hybrid B3LYP functional, the NL (D3) correction reproduces experimental and CCSD(T)/CBS dissociation energy with an error of 0.5(0.8) kcal mol⁻¹ and a MAD of 0.1(0.3) kcal mol⁻¹, respectively. All in all the two, methods show a similar trend in the calculation of (CH₂F₂)₂ dissociation energy, in agreement with the conclusions from previous benchmark studies,^{50,78} demonstrating that they treat dispersion correlation on solid physical grounds.

V. CONCLUSION

In the present work, difluoromethane and its homodimer have been investigated by infrared tunable diode laser spectroscopy coupled to quantum chemical calculations rooted in DFT.

The experimental measurements have been carried out around 8.1 μm, within the atmospheric region, and have led to the determination of the pressure broadening parameters and collisional cross sections for a number of difluoromethane ro-vibrational transitions, collisionally perturbed by noble gases (He, Ne, Ar), O₂, and N₂. The collisional cross sections have in turn been used for retrieving the dissociation energy of the (CH₂F₂)₂ dimer, which resulted 3.12 kcal mol⁻¹.

Theoretically, the dissociation energies corresponding to six stationary points on the potential energy surface of (CH₂F₂)₂ have been computed adopting various density functionals of the last generation. Specifically, the M06 suite of functionals (M06, M06-L, M06-2X, and M06-HF), three range separated functionals (LC-ωPBE, CAM-B3LYP, and ωB97X-D), as well as seven GGA- and hybrid-functionals (rPW86PBE, BLYP, revPBE, B3LYP, B3PW91, revPBE0, and revPBE38) augmented by the NL charge-density based dispersion correction have been considered in conjunction with different basis sets belonging to the families of Pople, Dunning, and Ahlrichs. The theoretical dissociation energies from these DFT calculations have been compared against either experimental data or reference values at the estimated CCSD(T)/CBS level. Among the tested functionals, LC-ωPBE, M06, and M06-L have yielded the worst results, with deviations from experiment up to (almost) 2 kcal mol⁻¹ and MADs from CCSD(T) reference values larger than 1 kcal mol⁻¹ with all the considered basis sets, but 6-311++G(*d*, *p*), which have led to better energies.

The Minnesota functionals M06-2X and M06-HF and the non-local vdW approach, especially when applied to rPW86PBE, BLYP, and B3LYP, have provided accurate energetics, reproducing the experimentally determined (CH₂F₂)₂ dissociation energy within 0.6 kcal mol⁻¹ as well as estimated CCSD(T)/CBS values with MADs lower than 0.4 kcal mol⁻¹. In particular, the performance of VV10 and B3LYP-NL is worth of note as these two functionals have reached the accuracy of the CCSD(T)/CBS correlated wavefunction method, providing MADs lower than 0.1 kcal mol⁻¹.

Summarizing, difluoromethane is a molecule of proved atmospheric relevance, whose atmospheric concentration has significantly increased during last years as a consequence of its commercial applications. It forms a dimer bonded through weak hydrogen bonds, in which the difluoromethane

fragments can act as a double proton donor and acceptor, respectively. On the one hand, N₂- and O₂- pressure broadening coefficients are of relevance for the reliable analysis of remote sensing spectroscopic measurements of our atmosphere, and on the other, it has been shown that collisional cross sections can also be employed for retrieving the dissociation energy of the homodimers. Theoretically, it has been shown that the reliable modelling of the (CH₂F₂)₂ dimer at DFT level requires the inclusion of dispersive forces into the Kohn-Sham density functional formalism. From this standpoint, the NL van der Waals correction, the Minnesota functionals M06-2X and M06-HF, and the atom pairwise dispersion correction D3 have demonstrated a high accuracy in describing the non-covalent interactions ruling the energetics of the stationary points on the PES of this complex.

ACKNOWLEDGMENTS

The High Performance Computing department of the CINECA Supercomputer Centre is gratefully acknowledged for the utilization of computer resources (Grant Nos. HP10CVN2S9 and HP10CVEVP7). This work has been supported by MIUR (PRIN 2012 funds for project “STAR: Spectroscopic and computational Techniques for Astrophysical and atmospheric Research”) and by University Ca’ Foscari Venezia. N.T. thanks University Ca’ Foscari Venezia for his post-doctoral position.

¹J.-M. Hartmann, C. Boulet, and D. Robert, *Collisional Effects on Molecular Spectra* (Elsevier, Amsterdam, 2008).

²G. Buffa, O. Tarrini, G. Cazzoli, and L. Dore, *Phys. Rev. A* **49**, 3557 (1994); G. Buffa, L. Dore, F. Tinti, and M. Meuwly, *ChemPhysChem* **9**, 2237 (2008); G. Buffa, O. Tarrini, L. Dore, and M. Meuwly, *ibid.* **11**, 3141 (2010).

³J.-M. Flaud, in *Spectroscopy from Space*, edited by J. Demaison, K. Sarka, and E. A. Cohen (Kluwer Academic Publisher, London, 1996), pp. 187–200; M. Herman, D. Hurtmans, and J. V. Auwera, in *Spectroscopy from Space*, edited by J. Demaison, K. Sarka, and E. A. Cohen (Kluwer Academic Publisher, London, 1996), pp. 201–218.

⁴K. G. Hay, S. Wright, G. Duxbury, and N. Langford, *Appl. Phys. B* **90**, 329 (2008).

⁵G. Duxbury, N. Langford, K. Hay, and N. Tasinato, *J. Mod. Opt.* **56**, 2034 (2009).

⁶M. R. Swain, G. Vasisht, and G. Tinetti, *Nature* **452**, 329 (2008).

⁷G. Tinetti, A. Vidal-Madjar, M.-C. Liang, J.-P. Beaulieu, Y. Yung, S. Carey, R. J. Barber, J. Tennyson, I. Ribas, N. Allard, G. E. Bellester, D. K. Sing, and F. Selsis, *Nature* **448**, 169 (2007).

⁸G. Cazzoli, L. Cludi, G. Cotti, C. D. Esposti, G. Buffa, and O. Tarrini, *J. Chem. Phys.* **102**, 1149 (1995).

⁹R. Ciuryło, D. A. Shapiro, J. R. Drummond, and A. D. May, *Phys. Rev. A* **65**, 012502 (2001).

¹⁰F. Thilbault, B. Corretja, D. Bermejo, R. Z. Martinez, and B. Bussery-Honvault, *Phys. Chem. Chem. Phys.* **10**, 5419 (2008).

¹¹F. Rohart, G. Włodarczak, J. M. Colmont, G. Cazzoli, L. Dore, and C. Puzzarini, *J. Mol. Spectrosc.* **251**, 282 (2008).

¹²N. Tasinato, G. Duxbury, N. Langford, and K. G. Hay, *J. Chem. Phys.* **132**, 044316 (2010).

¹³N. Tasinato, K. G. Hay, N. Langford, G. Duxbury, and D. Wilson, *J. Chem. Phys.* **132**, 164301 (2010); G. Duxbury, N. Tasinato, K. G. Hay, D. Wilson, and N. Langford, *AIP Conf. Proc.* **1290**, 194 (2010).

¹⁴N. Tasinato, G. Regini, P. Stoppa, A. P. Charmet, and A. Gambi, *J. Chem. Phys.* **136**, 214302 (2012).

¹⁵N. Tasinato, A. Turchetto, C. Puzzarini, P. Stoppa, A. P. Charmet, and S. Giorgianni, *Mol. Phys.* **112**, 2384 (2014).

¹⁶N. Tasinato, *Int. J. Quantum Chem.* **114**, 1472 (2014).

¹⁷J. Scaranto, D. Moro, N. Tasinato, P. Stoppa, and S. Giorgianni, *Spectrochim. Acta, Part A* **136**, 1614 (2014).

¹⁸W. Caminati, S. Melandri, P. Moreschini, and P. G. Favero, *Angew. Chem., Int. Ed.* **38**, 2924-2925 (1999).

- ¹⁹S. Blanco, J. C. López, A. Lesarri, and J. L. Alonso, *J. Mol. Struct.* **612**, 255 (2002).
- ²⁰A. Ebrahimi, H. Roohi, and S. M. Habibi, *J. Mol. Struct.: THEOCHEM* **684**, 87 (2004).
- ²¹N. Tasinato and S. Grimme, *Phys. Chem. Chem. Phys.* **17**, 5659 (2015).
- ²²P. Hobza, J. Sponer, and T. J. Reschel, *J. Comput. Chem.* **11**, 1315 (1995).
- ²³M. Allen and D. J. Tozer, *J. Chem. Phys.* **117**, 11113 (2002).
- ²⁴S. Kristyan and P. Pulay, *Chem. Phys. Lett.* **229**, 175 (1994).
- ²⁵S. Grimme, *ChemPhysChem* **12**, 1258 (2011).
- ²⁶S. Goerigk, H. Kruse, and S. Grimme, *ChemPhysChem* **12**, 211 (2011).
- ²⁷S. Grimme, *WIREs Comput. Mol. Sci.* **1**, 211 (2011).
- ²⁸J. Klimeš and A. Michaelides, *J. Chem. Phys.* **137**, 120901 (2012).
- ²⁹S. Grimme, *J. Comput. Chem.* **27**, 1787 (2006).
- ³⁰S. Grimme, J. Anthony, S. Ehrlich, and H. Krieg, *J. Chem. Phys.* **132**, 154104 (2010).
- ³¹K. Lee, E. D. Murray, L. Kong, B. I. Lundqvist, and D. C. Langreth, *Phys. Rev. B* **82**, 081101 (2010).
- ³²O. A. Vydrov and T. J. Van Voorhis, *J. Chem. Phys.* **133**, 244103 (2010).
- ³³Y. Zhao, N. E. Schultz, and D. G. Truhlar, *J. Chem. Theory Comput.* **2**, 364 (2006).
- ³⁴Y. Zhao and D. G. Truhlar, *Theor. Chem. Acc.* **120**, 215 (2008).
- ³⁵Y. Zhao and D. G. Truhlar, *J. Chem. Phys.* **125**, 194101 (2006).
- ³⁶Y. Zhao and D. G. Truhlar, *J. Phys. Chem. A* **110**, 13126 (2006).
- ³⁷T. Yanai, D. P. Tew, and N. C. Handy, *Chem. Phys. Lett.* **393**, 51 (2004).
- ³⁸O. A. Vydrov and G. E. Scuseria, *J. Chem. Phys.* **125**, 234109 (2006).
- ³⁹J.-D. Chai and M. Head-Gordon, *Phys. Chem. Chem. Phys.* **10**, 6615 (2008).
- ⁴⁰J. P. Perdew and W. Yue, *Phys. Rev. B* **33**, 8800 (1986); Erratum **40**, 3399 (1989).
- ⁴¹E. D. Murray, K. Lee, and D. C. Langreth, *J. Chem. Theory Comput.* **5**, 2754 (2009).
- ⁴²J. P. Perdew, K. Burke, and M. Ernzerhof, *Phys. Rev. Lett.* **77**, 3865 (1996).
- ⁴³A. D. Becke, *Phys. Rev. A* **38**, 3098 (1988).
- ⁴⁴C. Lee, W. Yang, and G. G. Parr, *Phys. Rev. B* **37**, 785 (1988).
- ⁴⁵Y. Zhang and W. Yang, *Phys. Rev. Lett.* **80**, 890 (1998).
- ⁴⁶A. D. Becke, *J. Chem. Phys.* **98**, 5648 (1993).
- ⁴⁷J. P. Perdew and Y. Wang, *Phys. Rev. B* **45**, 13244 (1992).
- ⁴⁸M. Ernzerhof and G. E. Scuseria, *J. Chem. Phys.* **110**, 5029 (1999).
- ⁴⁹C. Adamo and V. Barone, *J. Chem. Phys.* **110**, 6158 (1999).
- ⁵⁰W. Hujo and S. Grimme, *J. Chem. Theory Comput.* **7**, 3866 (2011); **9**, 308 (2013).
- ⁵¹R. Krishnan, J. S. Binkley, R. Seeger, and J. A. Pople, *J. Chem. Phys.* **72**, 650 (1980).
- ⁵²A. D. McLean and G. S. Chandler, *J. Chem. Phys.* **72**, 5639 (1980).
- ⁵³M. J. Frisch, J. A. Pople, and J. S. Binkley, *J. Chem. Phys.* **80**, 3265 (1984).
- ⁵⁴T. H. Dunning, Jr., *J. Chem. Phys.* **90**, 1007 (1989).
- ⁵⁵R. A. Kendall, T. H. Dunning, Jr., and R. J. Harrison, *J. Chem. Phys.* **96**, 6796 (1992).
- ⁵⁶D. E. Woon and T. H. Dunning, Jr., *J. Chem. Phys.* **98**, 1358 (1993).
- ⁵⁷E. R. Davidson, *Chem. Phys. Lett.* **260**, 514 (1996).
- ⁵⁸A. Schaefer, H. Horn, and R. Ahlrichs, *J. Chem. Phys.* **97**, 2571 (1992).
- ⁵⁹A. Schaefer, C. Huber, and R. Ahlrichs, *J. Chem. Phys.* **100**, 5829 (1994).
- ⁶⁰F. Weigend and R. Ahlrichs, *Phys. Chem. Chem. Phys.* **7**, 3297 (2005).
- ⁶¹M. J. Frisch, G. W. Trucks, H. B. Schlegel, G. E. Scuseria, M. A. Robb, J. R. Cheeseman, G. Scalmani, V. Barone, B. Mennucci, G. A. Petersson, H. Nakatsuji, M. Caricato, X. Li, H. P. Hratchian, A. F. Izmaylov, J. Bloino, G. Zheng, J. L. Sonnenberg, M. Hada, M. Ehara, K. Toyota, R. Fukuda, J. Hasegawa, M. Ishida, T. Nakajima, Y. Honda, O. Kitao, H. Nakai, T. Vreven, J. A. Montgomery, Jr., J. E. Peralta, F. Ogliaro, M. Bearpark, J. J. Heyd, E. Brothers, K. N. Kudin, V. N. Staroverov, R. Kobayashi, J. Normand, K. Raghavachari, A. Rendell, J. C. Burant, S. S. Iyengar, J. Tomasi, M. Cossi, N. Rega, J. M. Millam, M. Klene, J. E. Knox, J. B. Cross, V. Bakken, C. Adamo, J. Jaramillo, R. Gomperts, R. E. Stratmann, O. Yazyev, A. J. Austin, R. Cammi, C. Pomelli, J. W. Ochterski, R. L. Martin, K. Morokuma, V. G. Zakrzewski, G. A. Voth, P. Salvador, J. J. Dannenberg, S. Dapprich, A. D. Daniels, Ö. Farkas, J. B. Foresman, J. V. Ortiz, J. Cioslowski, and D. J. Fox, GAUSSIAN 09, Revision C.01, Gaussian, Inc., Wallingford, CT (2009).
- ⁶²F. Neese and F. Wennmohs, *ORCA - An ab initio, DFT and Semiempirical SCF-MO Package, Version 3.0.1* (Max-Planck-Institute for Chemical Energy Conversion, Germany, 2013).
- ⁶³F. Neese, *WIREs Comput. Mol. Sci.* **2**, 73 (2012).
- ⁶⁴R. Ahlrichs, *Phys. Chem. Chem. Phys.* **6**, 5119 (2004).
- ⁶⁵F. Weigend, M. Kattanneck, and R. Ahlrichs, *J. Chem. Phys.* **130**, 164106 (2009).
- ⁶⁶S. Kossmann and F. Neese, *Chem. Phys. Lett.* **481**, 240 (2009).
- ⁶⁷S. F. Boys and F. Bernardi, *Mol. Phys.* **19**, 553 (1970).
- ⁶⁸N. Tasinato, A. P. Charnet, P. Stoppa, S. Giorgianni, and G. Buffa, *J. Chem. Phys.* **132**, 044315 (2010).
- ⁶⁹N. Tasinato, A. P. Charnet, P. Stoppa, G. Buffa, and C. Puzzarini, *J. Quant. Spectrosc. Radiat. Transfer* **130**, 233 (2013).
- ⁷⁰N. Tasinato, P. Stoppa, A. P. Charnet, S. Giorgianni, G. Buffa, and A. Gambi, *ChemPhysChem* **12**, 356 (2011).
- ⁷¹N. Tasinato, A. P. Charnet, P. Stoppa, S. Giorgianni, and G. Buffa, *Spectrochim. Acta, Part A* **118**, 373 (2014).
- ⁷²N. Tasinato, A. P. Charnet, P. Stoppa, and S. Giorgianni, *Mol. Phys.* **108**, 677 (2010).
- ⁷³G. Cazzoli, L. Dore, C. Puzzarini, B. Bakri, J.-M. Colmont, F. Rohart, and G. Wlodarczak, *J. Mol. Spectrosc.* **229**, 158 (2005); J. M. Colmont, B. Bakri, F. Rohart, G. Wlodarczak, J. Demaison, G. Cazzoli, L. Dore, and C. Puzzarini, *ibid.* **231**, 171 (2005).
- ⁷⁴H.-M. Lin, M. Seaver, K. Y. Tang, A. E. W. Knight, and C. S. Parmenter, *J. Chem. Phys.* **70**, 5442 (1979).
- ⁷⁵H. R. Barry, L. Corner, G. Hancock, R. Peverall, T. L. Ranson, and G. A. D. Ritchie, *Phys. Chem. Chem. Phys.* **5**, 3106 (2003).
- ⁷⁶T. Nakayama, H. Fukuda, A. Sugita, S. Hashimoto, M. Kawasaki, S. Aloisio, I. Morino, and G. Inoue, *Chem. Phys.* **334**, 196 (2007).
- ⁷⁷See supplementary material at <http://dx.doi.org/10.1063/1.4916911> for the table of the binding energies for the (CH₂F₂)₂ conformers computed at DFT level.
- ⁷⁸W. Hujo and S. Grimme, *Phys. Chem. Chem. Phys.* **13**, 13942 (2011).